Magna Scientia Advanced Biology and Pharmacy
eISSN: 2582-8363
Cross Ref DOI: 10.30574/msabp
Journal homepage: https://msabp.magnascientiapub.com/

(RESEARCH ARTICLE)

DISTRIBUTION TREND OF HEAVY METALS AND PAHS IN SEDIMENT, POREWATER, AND WEST AFRICAN MUD CREEPER (*Tympanotomy falcatus var. radula*) FROM THE NIGER DELTA

Chinwe Fiona Anyanwu [1], Henry Eyina Dienye [2] and Davies Ibienebo Chris [2,*]

[1] Department of Pharmacology, University of Port Harcourt, East/West Road, Choba, Rivers State, PMB 5323, Nigeria.
[2] Department of Fisheries, University of Port Harcourt, East/West Road, Choba, Rivers State, PMB 5323, Nigeria.
* Corresponding Author

ORCID Details
Chinwe Fiona Anyanwu: https://orcid.org/0000-0002-0632-6306
Henry Eyina Dienye: https://orcid.org/0000-0001-6254-9179
Davies Ibienebo Chris: https://orcid.org/0000-0002-1722-7776

Magna Scientia Advanced Biology and Pharmacy, 2026, 19(01), 092–106

Publication history: Received on 11 September 2026; revised on 21 October 2026; accepted on 23 October 2026

Article DOI: https://doi.org/10.30574/msabp.2026.19.1.0079

Copyright © 2026 Author(s) retain the copyright of this article. This article is published under the terms of the Creative Commons Attribution License 4.0

ABSTRACT

Background: Petroleum-impacted Niger Delta creeks remain under-monitored, with few studies integrating sediment, porewater, and biota over time.

Methods: Heavy metals (Fe, Zn, Ni, Cd, Cr), total petroleum hydrocarbons (TPH) and the 16 US EPA priority polycyclic aromatic hydrocarbons (ΣPAH_{16}) were measured monthly from March to August 2026 at three stations along Bille Creek, Rivers State, Nigeria. Samples comprised surface sediment, interstitial water and soft tissue of *Tympanotonus fuscatus* var. radula. Porewater physicochemical parameters were also measured. Analyses used ICP-OES, ICP-MS, GC-FID and GC-MS, with certified reference materials and routine quality control.

Results: Sediment TPH peaked at 3,117.50 ± 10.14 mg/kg at Station 2, approximately 62 times the DPR EGASPIN sediment limit of 50 mg/kg. ΣPAH_{16} ranged from 11.78 to 40.27 mg/kg and exceeded the USEPA effects range-low (ERL; 4.0 mg/kg) at Stations 2 and 3. Sediment cadmium at Stations 1 and 2 (0.79 and 1.14 mg/kg) exceeded the CCME interim sediment quality guideline. Porewater TPH was highest in March (14.36 ± 2.04 mg/L) and stabilised at 1.80–2.00 mg/L from April to August. Nickel (0.21–0.22 mg/L) and iron (1.20–1.47 mg/L) exceeded WHO drinking-water guideline values at all stations. In *T. fuscatus*, tissue cadmium, lead, arsenic, TPH and ΣPAH increased from Station 1 to Station 3, and cadmium (0.050 to 0.100 mg/kg) and ΣPAH (0.006 to 0.011 mg/kg) increased between March and August.

Conclusions: The findings demonstrate persistent, spatially heterogeneous petroleum and metal contamination in Bille Creek, warranting pollution control and precautionary seafood safety measures.

Keywords: Biomonitoring; Bille Creek; Niger Delta; Heavy metals; PAH; *Tympanotonus fuscatus*; TPH; Sediment quality

1 INTRODUCTION

Coastal and deltaic waterways are under increasing pressure from industrial discharges, particularly where petroleum extraction and urban development lie close to ecologically sensitive estuarine habitats (Landrigan et al., 2020; Häder et al., 2020). Heavy metals and polycyclic aromatic hydrocarbons (PAHs) are among the most consequential contaminants because of their persistence, bioaccumulative potential and toxicity to aquatic organisms and human consumers (Abdel-Shafy & Mansour, 2016; Ali et al., 2019). Both partition from the water column into organic-rich sediments, which act as long-term sinks and secondary sources; under shifting redox potential, pH and salinity, bound metals and hydrocarbons can return to porewater and overlying water, sustaining benthic exposure long after primary discharges have ceased (ELTurk et al., 2019).

The Niger Delta is one of the most petroleum-affected deltaic systems in the world, its mangrove creeks and estuaries having received crude oil, produced water and combustion by-products from pipeline networks, flow stations and gas flaring over several decades (Ovutor & Brisibe, 2020). Documented consequences include mangrove loss, declines in artisanal fisheries and degraded benthic habitats (Ugochukwu & Lall, 2019). Human exposure through diet, dermal contact and inhalation has been associated with gastrointestinal, respiratory, neurological and reproductive effects in some epidemiological studies (Nriagu et al., 2016; Jaja-Chimedza et al., 2022).

Bille Creek, in the Degema Local Government Area of Rivers State, is a tidal tributary of the Sombrero River, surrounded by a community dependent on brackish mangrove creeks for fishing and shellfish harvesting. The creek lies near several petroleum facilities and was affected by a gas incident with associated chemical release reported by Obi (2021).

Most Niger Delta assessments characterise bulk sediment or surface water alone, with few reporting interstitial water chemistries alongside sediment and biota. This gap matters because the freely dissolved porewater fraction, rather than total sediment burden, largely controls bioavailability of metals and hydrocarbons to deposit-feeding benthos (Di Toro et al., 1991). Porewater speciation depends on acid-volatile sulfide (AVS)–metal equilibria, reductive dissolution of iron oxyhydroxides and organic-carbon normalisation of PAH partitioning, each sensitive to pH, redox potential, salinity, dissolved oxygen and organic loading (Di Toro et al., 1992). Integrating paired sediment, porewater and biota measurements over time is therefore a practical requirement for risk assessment in petroleum-impacted estuaries (MacDonald et al., 2000). Seasonal contrasts between the wet season (April–October) and dry season (November–March) also modulate dilution, remobilisation and bioaccumulation, which cross-sectional studies cannot capture (Nwankwoala, 2021).

Tympanotonus fuscatus (Linnaeus, 1758) is a dominant benthic gastropod of many West African estuarine and mangrove systems. As a sedentary deposit feeder with high sediment-ingestion rates and appreciable capacity for metal and hydrocarbon bioaccumulation, it is a sensitive indicator of benthic contamination and a vector of dietary exposure for communities harvesting it for protein and income (Barimalaa et al., 2020).

This study characterised the spatial and temporal distribution of Fe, Zn, Ni, Cd, Cr, TPH and ΣPAH_{16} in sediment, interstitial water and *T. fuscatus* soft tissue along Bille Creek over six months, together with key porewater physicochemical variables. Its objectives were to: (i) quantify spatial gradients among three stations in each matrix, evaluate monthly trend, examine physicochemical variables influencing contaminant mobility and bioavailability; and compare concentrations with sediment quality, water quality and food-safety reference values (USEPA ERL/ERM; CCME ISQG/PEL; DPR EGASPIN; WHO, 2022; FAO/WHO, 2011). To our knowledge, this is among the first paired sediment–porewater–biota time series for a petroleum-impacted creek in Rivers State, intended to inform monitoring, regulatory enforcement and remediation planning in Bille Creek and comparable Niger Delta estuaries.

2 MATERIALS AND METHODS

2.1 Study area

The study was conducted along Bille Creek, a tidal estuarine channel in the Degema Local Government Area of Rivers State, southern Nigeria (approximately 4°35′N, 6°45′E). Bille Creek is a tributary of the Sombrero River system, which discharges to the Atlantic Ocean through the Bight of Bonny (Obeka & Numbere, 2020). The adjacent landscape is brackish mangrove forest dominated by *Rhizophora racemosa*, *Avicennia germinans* and *Laguncularia racemosa*, with intertidal mudflats that support dense populations of *T. fuscatus* (Lawson, 2021). Petroleum infrastructure, including pipeline crossings and produced-water discharge points, lies along the creek. The region has a tropical humid climate, with a dry season from November to March and a wet season from April to October. Mean annual rainfall is 2,500–3,500 mm (Nwankwoala, 2021). Sampling therefore spanned the late dry season (March) and the wet season (April–August).

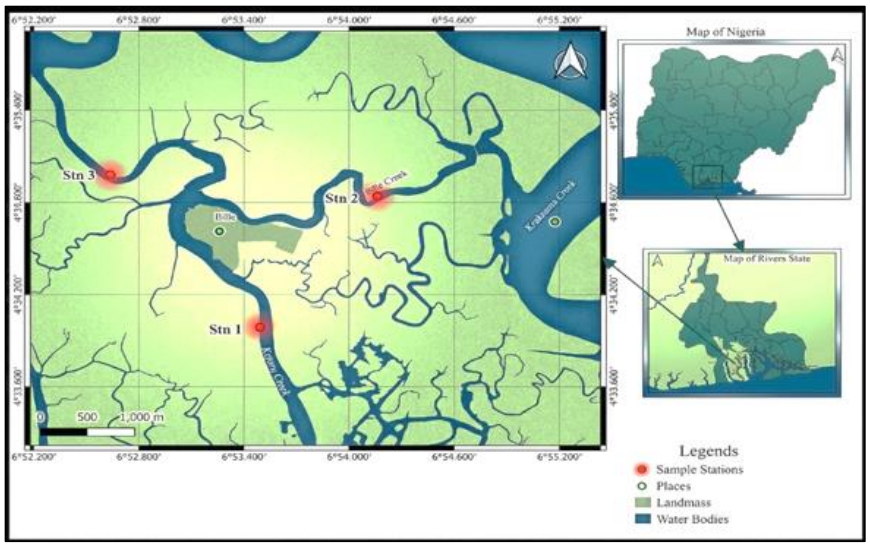


Figure 1: Map of the study area, showing the sampling sites along the Bille waterways.

2.2 Study design and station selection

Three stations were established along the creek using a stratified design informed by proximity to petroleum infrastructure, site accessibility and preliminary reconnaissance (Figure 1). Station 1 was the upstream reference, with intact mangrove vegetation and no direct discharge. Station 2 was nearest to the petroleum facility associated with the reported gas incident and showed pipeline crossings and hydrocarbon staining on intertidal sediments. Station 3 lay downstream of the primary discharge zone, where fine-grained sediments are expected to accumulate under tidal and fluvial hydrodynamics.

Within each station, three sub-stations (1, 2 and 3) were located approximately 50 m apart, perpendicular to the channel axis. Station coordinates were recorded with a handheld GPS receiver referenced to WGS84.

2.3 Sampling schedule

Sampling was conducted monthly from March to August 2026. Each sampling event occurred at mid-ebb tide to reduce tidal confounding (ELTurk et al., 2019). At each sub-station, one composite sediment sample, one porewater sample set and one composite *T. fuscatus* sample were collected. The sub-station was the unit of replication, giving n = 3 per station per month for each matrix. Across six months and three stations, this yielded 54 sediment, 54 porewater and 54 tissue samples.

2.4 Sediment collection and preparation

Surface sediment (0–10 cm) was collected from intertidal mudflats using a stainless-steel Ekman grab (0.025 m^2). Three grabs within a 2 m radius were homogenised in the field to form one composite per sub-station, stored in pre-cleaned 500 mL amber borosilicate jars with PTFE-lined lids, transported on ice to the laboratory within 6 h, and held at −20 °C until analysis.

In the laboratory, samples were homogenised with a stainless-steel spatula and macrofauna, shell fragments and coarse debris removed. Subsamples for metal analysis were air-dried, oven-dried at 60 °C to constant mass, disaggregated in an agate mortar, and sieved through a 63 µm stainless-steel mesh to isolate the fine fraction, the principal carrier phase for sorbed metals and hydrophobic organic contaminants (Förstner & Wittmann, 2012; MacDonald et al., 2000).

For physicochemical characterisation, pH was measured in the field, or within 2 h of collection, on a wet subsample (~100 g) using a glass combination electrode (Hanna HI 9025) calibrated with NIST-traceable buffers (pH 4.0, 7.0 and 10.0). Electrical conductivity was measured with a HACH HQ40d meter. Total organic carbon (TOC) was determined on dried, acidified (10% HCl) subsamples by CHNS/O elemental analysis (Elementar vario MACRO cube), and total available phosphorus colorimetrically after alkaline persulfate digestion (APHA Method 4500-P; APHA, 2017).

2.5 Interstitial water collection and preparation

Interstitial water was extracted from undisturbed sediment cores (15 cm long, 7 cm i.d.) collected with hand-held polycarbonate tubes fitted with rubber end caps. Cores were sealed, transported upright on ice, and processed within 4 h. In the laboratory, cores were extruded under nitrogen in a glove bag to limit oxidation of redox-sensitive species

(Di Toro et al., 1992). The upper 0–10 cm was transferred to pre-cleaned 50 mL polypropylene tubes and centrifuged at 3,500 rpm for 30 min at 4 °C (Eppendorf 5810R). The supernatant was decanted under nitrogen and filtered through 0.45 µm cellulose acetate membranes.

Filtered porewater was split into three aliquots: (i) metals, acidified to pH <2 with ultrapure HNO_3 and stored at 4 °C in HDPE vials; (ii) TPH and PAHs, stored in amber PTFE-capped glass vials at −20 °C; and (iii) physicochemical and ionic analyses, stored unacidified at 4 °C and analysed within 48 h.

Turbidity was measured with a calibrated HACH 2100AN turbidimeter (FNU), TDS gravimetrically (APHA 2540C), salinity from conductivity on the Practical Salinity Scale (dimensionless), and DO in the field using a YSI Pro20 polarographic probe. Total alkalinity was determined by potentiometric titration with 0.02 N H_2SO_4 to pH 4.5 (APHA 2320B), BOD_5 by the five-day method at 20 °C (APHA 5210B), and COD by open-reflux dichromate digestion (APHA 5220B).

2.6 *Tympanotonus fuscatus* collection and tissue preparation

Specimens of *T. fuscatus* (Linnaeus, 1758) were hand-collected at low tide from randomly placed 1 m × 1 m quadrats in the intertidal zone of each sub-station (Ndome et al., 2012; Lawson, 2021). At least 30 sexually mature adults of comparable size (25–40 mm shell length) were collected per sub-station monthly, kept on ice, and processed within 6 h.

Shell length was measured with a digital vernier caliper and wet mass with an analytical balance. Specimens were rinsed three times with ultrapure water (18.2 MΩ·cm) to remove adhering sediment, and soft tissues (foot, mantle, gill and visceral mass) were extracted with pre-cleaned stainless-steel tools. Tissues were pooled into one composite sample per sub-station per month to account for inter-individual variation (Afiukwa et al., 2020), frozen at −80 °C, freeze-dried to constant mass, ground in an agate ball mill, and stored at −20 °C in sealed amber vials.

2.7 Heavy metal analysis

Sediment digestion followed USEPA Method 3051A. Approximately 0.5 g of dried, sieved sediment was digested in PTFE vessels with 9 mL concentrated HNO_3 (65%, Suprapur) and 3 mL concentrated HCl (37%, Suprapur) in a microwave system (Anton Paar Multiwave Pro), ramped to 120 °C (held 5 min), then to 175 °C (held 10 min). Digestates were filtered through Whatman No. 42 paper, diluted to 50 mL with ultrapure water, and analysed (USEPA, 2007).

Tissue (0.3 g dry mass) was digested using the same protocol with 6 mL HNO_3 and 2 mL H_2O_2 (30%, Suprapur) to oxidise organic matter (USEPA, 2007). Porewater metals were analysed directly after acidification, using matrix-matched calibration standards in 2% HNO_3.

Elements were quantified by ICP-OES (PerkinElmer Optima 8300) and ICP-MS (PerkinElmer NexION 350D) following APHA Method 3120B and USEPA Method 6020A (APHA, 2017; USEPA, 2014), with ICP-MS used for low-concentration elements, particularly cadmium in porewater, requiring lower detection limits. Calibration curves (0.01–10 mg/L) were prepared from certified standards (Merck Certipur) with $r^2 > 0.9999$, and online internal standards (^{115}In and ^{205}Tl) corrected for drift and matrix effects.

2.8 TPH and PAH analysis

- **Sediment**: Freeze-dried sediment (~10 g) was spiked with deuterated PAH surrogates (naphthalene-d_8, acenaphthylene-d_{10}, phenanthrene-d_{10}, chrysene-d_{12} and perylene-d_{12}; AccuStandard) and ultrasonically extracted (USEPA Method 3550C) with 100 mL of 1:1 (v/v) dichloromethane (DCM): acetone in three 15-min cycles. Extracts were dried over anhydrous Na_2SO_4, concentrated by rotary evaporation and nitrogen blow-down, and reconstituted in hexane. Cleanup used silica SPE cartridges (1 g); aliphatic TPH was eluted with 10 mL hexane and PAHs with 10 mL of 20% DCM in hexane.
- **Porewater**: Surrogates were added to samples (up to 100 mL) before liquid–liquid extraction with three 30 mL portions of DCM (USEPA Method 3510C). Extracts were dried, concentrated and cleaned up by the same SPE procedure.
- **Tissue**: Freeze-dried tissue (~2 g) was saponified with 50 mL of 0.5 M ethanolic KOH at 70 °C for 2 h under reflux to hydrolyse lipids (Barimalaa et al., 2020). Surrogates were added after cooling, and the digest was extracted with three 30 mL portions of DCM, washed with ultrapure water to remove residual KOH, dried and cleaned up by SPE.
- **Instrumental analysis**: TPH was quantified by GC-FID (Agilent 7890B) with a DB-5 column (30 m × 0.32 mm × 0.25 µm) following USEPA Method 8015D, using an oven programme of 50 °C (2 min hold), ramped at 10 °C min^{-1} to 300 °C (10 min hold), and calibrated against a C_8–C_{40} alkane standard (Supelco). The 16 USEPA priority PAHs were quantified by GC-MS (Agilent 7890B/5977B) in selected-ion monitoring mode following USEPA

Method 8270E, with an oven programme of 60 °C (1 min hold), ramped at 8 °C min^{-1} to 310 °C (15 min hold). Individual PAHs were quantified by isotope-dilution calibration against the deuterated surrogates and summed to ΣPAH_{16} (Abdel-Shafy & Mansour, 2016; Samanta et al., 2022).

2.9 Quality assurance and quality control

Field blanks (ultrapure water handled as samples) and method blanks (one per batch of 10 samples) monitored contamination. Analytical accuracy was verified with certified reference materials in each batch: NIST SRM 2702 (marine sediment) for sediment and NIST SRM 1566b (*T. fuscatus* tissue) for biota. Deuterated surrogate recoveries were required to fall between 70% and 130%. Matrix spike/spike duplicates (one per 10 samples) required recoveries of 80–120%. Field and laboratory duplicates (10% frequency) required relative percent differences below 20%. Instrument calibration was checked at the start of each run and every ten samples. Method detection limits were three times the standard deviation of seven replicate low-level standards, and values below the MDL were reported as < MDL. Instrument detection limits were 0.001 mg/L (ICP-OES), 0.0001 mg/L (ICP-MS), 0.01 mg/kg (GC-FID, TPH) and 0.001 mg/kg (GC-MS, PAHs).

2.10 Statistical analysis

Analyses were performed in IBM SPSS Statistics 28.0 and R 4.3.1 (R Core Team, 2023). Normality was assessed with the Shapiro–Wilk test (Shapiro & Wilk, 1965; applied for $n < 50$) and homogeneity of variance with Levene's test. Variables violating normality ($p < 0.05$) were $\log_{10}$-transformed or analysed non-parametrically. Spatial differences among stations and temporal differences among months were tested by one-way analysis of variance (ANOVA), with station or month as fixed factors. Where the ANOVA was significant, Tukey's HSD test was used for pairwise comparisons. Significance was set at $\alpha = 0.05$, with $p < 0.01$ and $p < 0.001$ denoted as highly and very highly significant.

3 RESULTS AND DISCUSSION

3.1 Spatial distribution in sediment

TPH in sediment differed strongly among stations (Table 1; $p < 0.001$), averaging 20.67 ± 1.89 mg/kg at Station 1, 3,117.50 ± 10.14 mg/kg at Station 2 and 2,097.50 ± 8.50 mg/kg at Station 3. The Station 2 value was ~62 times the DPR EGASPIN sediment limit of 50 mg/kg (DPR, 2002). This pattern, peaking at the facility-adjacent station and attenuating downstream, is consistent with a point-source geometry (Neff et al., 2011). Station 1 exceeded background levels for pristine tropical estuarine sediments (<5 mg/kg) (Readman et al., 2002), suggesting diffuse atmospheric deposition and tidal redistribution rather than direct discharge.

ΣPAH_{16} followed the same gradient, declining from 40.27 ± 0.33 mg/kg at Station 2 to 31.42 ± 0.42 mg/kg at Station 3 and 11.78 ± 17.42 mg/kg at Station 1 ($p < 0.001$). Stations 2 and 3 exceeded the USEPA ERL of 4.0 mg/kg and approached the effects range-median (ERM; 44.8 mg/kg), above which adverse effects are frequently observed (Long et al., 1995). Comparable concentrations (15–38 mg/kg) have been reported in petroleum-impacted estuaries of Edo State (Ezemonye et al., 2021). The large standard deviation at Station 1 (CV 148%; mean 11.78, SD 17.42 mg/kg) indicates a patchy, highly skewed distribution in the upstream fringe, likely controlled by sediment texture and organic carbon rather than source proximity, and better described by median and interquartile range.

Iron was the dominant metal at all stations (3,626.67 ± 31.97, 3,973.33 ± 16.33 and 3,306.67 ± 16.33 mg/kg at Stations 1, 2 and 3; $p < 0.001$), consistent with the naturally iron-rich lateritic geology, with possible additional inputs from corrosion products and drilling residues (Nwankwoala, 2021; Neff et al., 2011). Iron oxyhydroxides are major binding phases for Cd, Zn, Ni and Cr, and their reductive dissolution under low-oxygen, organic-rich conditions at Stations 2 and 3 could release these metals to porewater, although this mechanism was inferred, not measured directly.

Zinc increased from Station 1 (38.48 ± 0.49 mg/kg) to Station 3 (45.48 ± 0.49 mg/kg) and Station 2 (49.48 ± 0.49 mg/kg; $p < 0.001$). All stations were below the CCME ISQG (123 mg/kg) and USEPA ERL (150 mg/kg) (Long et al., 1995; CCME, 1999), but exceeded the USEPA background reference (35 mg/kg) for coastal sediments (USEPA, 2023), indicating anthropogenic enrichment. Nickel showed the reverse gradient, declining from Station 1 (6.75 ± 0.10 mg/kg) to Station 2 (5.73 ± 0.10 mg/kg) and Station 3 (4.25 ± 0.13 mg/kg; $p < 0.05$), attributed to retention in organic-rich, fine-grained upstream sediments (TOC = 6.95%) rather than direct discharge. All values were below the CCME ISQG (15.9 mg/kg) and USEPA ERL (20.9 mg/kg).

Cadmium was the most ecotoxicologically significant metal, peaking at Station 2 (1.14 ± 0.05 mg/kg), followed by Station 1 (0.79 ± 0.10 mg/kg) and Station 3 (0.19 ± 0.05 mg/kg; $p < 0.001$). Stations 1 and 2 exceeded the CCME ISQG for cadmium, but were below the USEPA ERL (1.2 mg/kg; Long et al., 1995). Enrichment at Station 2 is consistent with

co-located petroleum infrastructure, although source apportionment was not performed, while the decline at Station 3 is consistent with sulfide precipitation and dilution (Di Toro et al., 1992).

Chromium decreased from Station 1 (12.74 ± 0.10 mg/kg) to Station 2 (10.88 ± 0.10 mg/kg) and Station 3 (9.64 ± 0.10 mg/kg; $p < 0.01$), consistent with geogenic background and diffuse atmospheric input rather than point discharge. All values were below the CCME ISQG (37.3 mg/kg) and USEPA ERL (81 mg/kg). Cr(III) and Cr(VI) were not speciated; oxidation of Cr(III) by manganese oxides in oxidised surface sediments is a recognised pathway requiring investigation (Masindi & Muedi, 2018)

Table 1: Mean ± SD sediment concentrations of metals, TPH and ΣPAH_{16} by station, averaged across all six months (dry-weight basis).

PARAMETERS	Station 1 (Mean ± SD)	Station 2 (Mean ± SD)	Station 3 (Mean ± SD)	Significance
TPH (mg/kg)	20.67 ± 1.89	3117.50 ± 10.14	2097.50 ± 8.50	***
PAH (mg/kg)	11.78 ± 17.42	40.27 ± 0.33	31.42 ± 0.42	***
Zinc, Zn (mg/kg)	38.48 ± 0.49	49.48 ± 0.49	45.48 ± 0.49	***
Nickel, Ni (mg/kg)	6.75 ± 0.10	5.73 ± 0.10	4.25 ± 0.13	*
Cadmium, Cd (mg/kg)	0.79 ± 0.10	1.14 ± 0.05	0.19 ± 0.05	***
Iron, Fe (mg/kg)	3626.67 ± 31.97	3973.33 ± 16.33	3306.67 ± 16.33	***
Chromium, Cr (mg/kg)	12.74 ± 0.10	10.88 ± 0.10	9.64 ± 0.10	**

Notes: Significance: Values represent Mean ± Standard Deviation; *** = $p < 0.001$; ** = $p < 0.01$; * = $p < 0.05$; Station 1, Station 2, Station 3 = Average of stations across all 6 months.

3.2 Temporal variation in sediment

Sediment TPH increased significantly over the six months (Table 2; $p < 0.001$), from 24.31 ± 4.78 mg/kg in March to 30.38 ± 5.83 mg/kg in August, a 25% net increase. Most of this occurred in the final month, which should be interpreted with caution given the few sampling occasions; the August value is an outlier relative to April–July. Reduced tidal flushing during the drying phase (July–August) would be expected to favour accumulation of hydrocarbon-laden fine particles (ELTurk et al., 2019).

Table 2: Monthly sediment concentrations (mean ± SD) of TPH, ΣPAH_{16} and metals.

PARAMETERS	March	April	May	June	July	August	Significance
TPH (mg/kg)	24.311 ± 4.781	25.183 ± 4.895	25.283 ± 4.907	25.333 ± 4.915	25.383 ± 4.923	30.383 ± 5.825	***
PAH (mg/kg)	39.867 ± 3.959	25.650 ± 16.819	25.817 ± 16.913	25.900 ± 16.979	25.967 ± 17.031	26.567 ± 17.532	***
Zinc, Zn (mg/kg)	45.050 ± 5.070	44.050 ± 4.905	44.150 ± 4.919	44.200 ± 4.926	44.250 ± 4.933	44.300 ± 4.941	NS
Nickel, Ni (mg/kg)	5.617 ± 1.049	5.517 ± 1.031	5.417 ± 1.012	5.367 ± 1.004	5.317 ± 0.996	5.217 ± 0.978	*
Cadmium, Cd (mg/kg)	0.763 ± 0.380	0.757 ± 0.379	0.700 ± 0.358	0.653 ± 0.335	0.607 ± 0.312	0.560 ± 0.291	NS
Iron, Fe (mg/kg)	3641.667 ± 293.017	3628.333 ± 290.816	3638.333 ± 292.269	3635.000 ± 291.822	3633.333 ± 291.537	3630.000 ± 291.091	NS
Chromium, Cr (mg/kg)	11.233 ± 1.649	11.133 ± 1.633	11.150 ± 1.636	11.150 ± 1.636	11.183 ± 1.641	11.233 ± 1.649	NS

Legend: Values represent Mean ± Standard Deviation across all 9 samples (Stations 1, 2, 3) per month.; Significance: *** = $p < 0.001$; ** = $p < 0.01$; * = $p < 0.05$; NS = Not Significant ($p > 0.05$); ND = No Data / Parameter not measured in March; <0.001 = Below detection limit; Key Findings: TPH, PAH, and Nickel show significant temporal variations across months

ΣPAH_{16} was highest in March (39.87 ± 3.96 mg/kg), fell to ~25–26 mg/kg from April onward, and rose slightly to 26.57 ± 17.53 mg/kg in August ($p < 0.001$). The March peak coincides with the reported gas incident (Obi, 2021), when

pyrogenic PAHs from combustion would be expected. The subsequent decline is consistent with microbial degradation of lighter PAHs, tidal redistribution and dilution (Samanta et al., 2022), a pattern of initial spike followed by incomplete attenuation also described in other estuaries (Vane et al., 2020). The lowest monthly mean (25.65 mg/kg in April) still exceeded the USEPA ERL of 4.0 mg/kg, indicating persistent ecotoxicological risk throughout the study. Large standard deviations from April onward (16.8–17.5 mg/kg) reflect spatial heterogeneity among stations.

Zn, Fe, Cd and Cr showed no significant monthly variation ($p > 0.05$; Table 2). Nickel declined modestly from 5.62 ± 1.05 mg/kg in March to 5.22 ± 0.98 mg/kg in August ($p < 0.05$), possibly reflecting dilution of nickel-enriched fine sediment by wet-season flushing. Overall, bulk metal concentrations were temporally stable, whereas hydrocarbon burdens rose or persisted above risk thresholds.

3.3 Spatial distribution in interstitial water

Porewater TPH was highest at Station 1 (5.67 ± 8.26 mg/L), followed by Station 2 (3.29 ± 0.06 mg/L) and Station 3 (2.27 ± 0.07 mg/L) (Table 3). The Station 1 mean was driven by a single high value (17.04 mg/L in July) and based only on July–August data, conflicting with the description of Table 3 means as "across all 6 months." As Station 1 is the reference station, this anomaly is discussed in Section 3.4. All values exceeded the study reference values; even the lowest mean (Station 3) exceeded 0.01 and 0.05 mg/L by 227- and 45-fold, respectively, but fell within the range reported near oilfield flow stations in Okirika, Niger Delta (1.8–6.4 mg/L) (Nwipie et al., 2019).

PAHs were below detection (<0.001 mg/L) at all stations throughout, consistent with strong sorption of four- to six-ring PAHs to sediment organic carbon (log K_oc > 4.5), keeping dissolved concentrations low despite high sediment concentrations (Abdel-Shafy & Mansour, 2016). Sediment ingestion is therefore the probable PAH exposure route for *T. fuscatus*.

Cadmium averaged 0.04 mg/L at all stations, with no spatial gradient but high variability (CV 100–125%), reflecting episodic pulses rather than a spatial pattern. Values reached 0.098–0.160 mg/L in April, with a secondary increase at Station 3 in August (0.111–0.113 mg/L), possibly from release from iron oxyhydroxides under transient anoxia (Di Toro et al., 1992). Mean cadmium exceeded the WHO drinking-water guideline (0.003 mg/L) ~13-fold and the DPR limit (0.01 mg/L) ~4-fold.

Dissolved iron increased downstream from 1.20 ± 0.01 mg/L (Station 1) to 1.24 ± 0.01 mg/L (Station 2) and 1.47 ± 0.03 mg/L (Station 3; $p < 0.001$), opposite to sediment iron and consistent with reductive dissolution of ferric oxyhydroxides downstream, where organic carbon is higher (Berner, 1980). All stations exceeded the WHO aesthetic guideline (0.30 mg/L), and Station 3 approached the DPR surface-water limit (1.0 mg/L) (DPR, 2002). Chromium also increased downstream (0.030 ± 0.000 to 0.034 ± 0.001 and 0.039 ± 0.001 mg/L; $p < 0.001$), but remained below the WHO/DPR limit (0.05 mg/L); speciation is required, however, as total chromium does not distinguish toxic Cr(VI).

Zinc (0.13–0.15 mg/L) was below WHO and DPR values (3.0 and 5.0 mg/L), whereas dissolved nickel (0.21–0.22 mg/L) exceeded the WHO guideline (0.07 mg/L) and DPR limit (0.10 mg/L) (WHO, 2022; DPR, 2002) despite sediment nickel being below ISQG and ERL thresholds, underlining the importance of porewater measurements for exposure assessment.

Table 3: Mean ± SD interstitial water concentrations by station (mg/L).

PARAMETERS	Station 1 (Mean ± SD)	Station 2 (Mean ± SD)	Station 3 (Mean ± SD)
TPH (mg/L)	5.67 ± 8.26*	3.29 ± 0.06	2.27 ± 0.07
PAH (mg/L)	<0.001	<0.001	<0.001
Cadmium, Cd (mg/L)	0.04 ± 0.04**	0.04 ± 0.05**	0.04 ± 0.05**
Zinc, Zn (mg/L)	0.13 ± 0.001	0.14 ± 0.001	0.15 ± 0.003
Nickel, Ni (mg/L)	0.22 ± 0.002	0.22 ± 0.001	0.21 ± 0.002
Iron, Fe (mg/L)	1.20 ± 0.01***	1.24 ± 0.01***	1.47 ± 0.03***
Chromium, Cr (mg/L)	0.030 ± 0.000***	0.034 ± 0.001***	0.039 ± 0.001***

Notes: Station 1, Station 2, Station 3 = Average of stations across all 6 months; Values represent Mean ± Standard Deviation; <0.001 indicates below detection limit.

3.4 Temporal variation in interstitial water

Porewater TPH was highest in March (14.36 ± 2.04 mg/L), fell by approximately 87% in April (1.80 ± 1.47 mg/L), and remained between 1.80 and 2.00 mg/L through August ($p < 0.001$; Table 4). The March peak coincides with the reported gas incident and is consistent with the pulse of soluble and semi-volatile hydrocarbons that infiltrates sediment porewater during acute spills (Neff et al., 2011). Its attenuation from April onward likely reflects microbial degradation, tidal flushing and loss of the most soluble fractions (Samanta et al., 2022). The persistence of TPH at 1.80–2.00 mg/L after the pulse indicates a chronic background burden, which exceeded the reference values used in this study by factors of approximately 180 (against 0.01 mg/L) and 36 (against 0.05 mg/L).

PAHs remained below detection throughout. Even at the March TPH peak, the aromatic fraction stayed in the sediment phase, which is consistent with the high organic-carbon partition coefficients of these compounds.

Dissolved zinc (0.1403 ± 0.0090 mg/L) and nickel (0.2170 ± 0.0045 mg/L) were reported as identical across all six months. Concentrations were therefore temporally stable, consistent with sulfide buffering, and exceedances for nickel were persistent throughout the year.

Iron and chromium were measured only in July (1.280 ± 0.130 mg/L and 0.0343 ± 0.0038 mg/L). These values confirm the spatial results but do not allow a temporal analysis. This is a monitoring gap that future work should close.

Table 4: Monthly interstitial water concentrations (mean ± SD; mg/L).

PARAMETERS	March	April	May	June	July	August
TPH (mg/L)	14.359 ±2.041	1.803 ±1.470	1.970 ±1.631	1.980 ±1.642	1.983 ±1.645	1.997 ±1.659
PAH (mg/L)	<0.001	<0.001	<0.001	<0.001	<0.001	<0.001
Zinc, Zn (mg/L)	0.1403 ±0.0090	0.1403 ±0.0090	0.1403 ±0.0090	0.1403 ±0.0090	0.1403 ±0.0090	0.1403 ±0.0090
Nickel, Ni (mg/L)	0.2170 ±0.0045	0.2170 ±0.0045	0.2170 ±0.0045	0.2170 ±0.0045	0.2170 ±0.0045	0.2170 ±0.0045
Iron, Fe (mg/L)	ND	ND	ND	ND	1.280 ±0.130	ND
Chromium, Cr (mg/L)	ND	ND	ND	ND	0.0343 ±0.0038	ND

Legend: Significance: *** = $p < 0.001$; ** = $p < 0.01$; * = $p < 0.05$; NS = Not Significant ($p > 0.05$), ND = No Data / Parameter not measured in that month, <0.001 = Below detection limit

3.5 Spatial distribution in *Tympanotonus fuscatus* soft tissue

Table 5: Mean ± SD concentrations in *T. fuscatus* soft tissue by station (mg/kg dry weight)

PARAMETERS	Station 1	Station 2	Station 3	Significance
TPH (mg/kg)	0.168 ± 0.009	0.188 ± 0.009	0.208 ± 0.009	***
PAH (mg/kg)	0.005 ± 0.002	0.008 ± 0.002	0.011 ± 0.002	***
Cadmium, Cd (mg/kg)	0.037 ± 0.017	0.070 ± 0.017	0.103 ± 0.017	***
Copper, Cu (mg/kg)	1.648 ± 0.167	1.848 ± 0.167	2.048 ± 0.167	***
Zinc, Zn (mg/kg)	42.5 ± 1.708	47.5 ± 1.708	52.5 ± 1.708	***
Lead, Pb (mg/kg)	0.082 ± 0.027	0.120 ± 0.027	0.158 ± 0.027	***
Arsenic, As (mg/kg)	0.052 ± 0.020	0.085 ± 0.020	0.118 ± 0.020	***
Iron, Fe (mg/kg)	330.0 ± 17.08	370.0 ± 17.08	410.0 ± 17.08	***

Significance: *** = $p < 0.001$ (Highly Significant). All parameters show highly significant differences across the three stations while Station 1 < Station 2 < Station 3 (indicating increasing contamination levels)

All eight tissue parameters (TPH, ΣPAH_{16}, Cd, Cu, Zn, Pb, As and Fe) increased from Station 1 to Station 3 (Table 5; all $p < 0.001$). TPH rose from 0.168 ± 0.009 to 0.208 ± 0.009 mg/kg (23.8%), while ΣPAH rose from 0.005 ± 0.002 to 0.011 ±

0.002 mg/kg (120%). As PAHs are accumulated mainly from ingested sediment, this steeper increase is consistent with higher PAH concentrations in Station 2 and 3 sediments (Table 1) (Neff et al., 2011; Barimalaa et al., 2020).

Cadmium increased nearly three-fold, from 0.037 ± 0.017 mg/kg at Station 1 to 0.103 ± 0.017 mg/kg at Station 3 (Station 2: 0.070 ± 0.017 mg/kg). The Station 3 value is below the FAO/WHO maximum level for cadmium in molluscs (0.5 mg/kg) (FAO/WHO, 2011), but among the higher *T. fuscatus* values reported in the Niger Delta (Barimalaa et al., 2020; Lawson, 2021), probably due to metallothionein binding in the digestive gland (Afiukwa et al., 2020).

Lead increased from 0.082 ± 0.027 to 0.158 ± 0.027 mg/kg (92.7%; $p < 0.001$), below the FAO/WHO maximum for shellfish (0.30 mg/kg). Arsenic rose from 0.052 ± 0.020 mg/kg at Station 1 to 0.118 ± 0.020 mg/kg at Station 3 (126.9%; $p < 0.001$), below the FAO/WHO total arsenic maximum for seafood (1.0 mg/kg), although speciation is needed to assess carcinogenic risk, as total arsenic does not distinguish inorganic arsenic from arsenobetaine.

Copper increased from 1.648 ± 0.167 to 2.048 ± 0.167 mg/kg, and zinc from 42.5 ± 1.71 to 52.5 ± 1.71 mg/kg. Both are essential, homeostatically regulated elements and remained below FAO/WHO reference values for shellfish (30 mg/kg for Cu; 40–100 mg/kg for Zn). Iron was the dominant metal (330.0 ± 17.08, 370.0 ± 17.08 and 410.0 ± 17.08 mg/kg), with bioaccumulation factors relative to porewater of ~275, 298 and 279, within the range reported for this species in Okirika and Ondo State (Nwipie et al., 2019; Lawson, 2021).

3.6 Temporal variation in *Tympanotonus fuscatus* soft tissue

Every tissue parameter increased significantly between March and August (Table 6; all $p < 0.001$). TPH rose from 0.170 to 0.205 mg/kg (20.6%; 0.0074 mg/kg per month; $r^2 = 0.963$), and ΣPAH from 0.006 to 0.011 mg/kg (83.3%; 0.0010 mg/kg per month; $r^2 = 0.953$).

Cadmium doubled from 0.050 ± 0.030 mg/kg in March to 0.100 ± 0.030 mg/kg in August (100%; 0.010 mg/kg per month; $r^2 = 0.952$; $p < 0.001$), the highest proportional change among the metals. Linear extrapolation would give ~0.22 mg/kg after 12 months, still below the FAO/WHO maximum (0.5 mg/kg). However, as cadmium is nephrotoxic and carcinogenic, and the study population includes women of reproductive age and children, a trend of this magnitude warrants precautionary action (WHO, 2022; Nriagu et al., 2016).

Table 6: Monthly *T. fuscatus* soft tissue concentrations (mg/kg dry weight; mean ± SD).

PARAMETERS	March	April	May	June	July	August	Sign
TPH (mg/kg)	0.170 ± 0.013	0.181 ± 0.013	0.192 ± 0.013	0.197 ± 0.013	0.197 ± 0.013	0.205 ± 0.013	***
PAH (mg/kg)	0.006 ± 0.003	0.007 ± 0.003	0.009 ± 0.003	0.010 ± 0.003	0.010 ± 0.003	0.011 ± 0.003	***
Cadmium, Cd (mg/kg)	0.050 ± 0.030	0.061 ± 0.030	0.080 ± 0.030	0.090 ± 0.030	0.090 ± 0.030	0.100 ± 0.030	***
Copper, Cu (mg/kg)	1.700 ± 0.200	1.800 ± 0.200	1.900 ± 0.200	1.950 ± 0.200	1.950 ± 0.200	2.000 ± 0.200	***
Zinc, Zn (mg/kg)	44.0 ± 3.464	45.0 ± 3.464	47.0 ± 3.464	48.0 ± 3.464	48.0 ± 3.464	49.0 ± 3.464	***
Lead, Pb (mg/kg)	0.090 ± 0.030	0.100 ± 0.030	0.120 ± 0.030	0.130 ± 0.030	0.130 ± 0.030	0.140 ± 0.030	***
Arsenic, As (mg/kg)	0.060 ± 0.030	0.070 ± 0.030	0.090 ± 0.030	0.100 ± 0.030	0.100 ± 0.030	0.110 ± 0.030	***
Iron, Fe (mg/kg)	340.0 ± 30.55	350.0 ± 30.55	370.0 ± 30.55	380.0 ± 30.55	380.0 ± 30.55	390.0 ± 30.55	***

Legend: Values represent Mean ± Standard Deviation across all 9 samples per month; F-value: One-way ANOVA test statistic comparing the six months; Significance: *** = $p < 0.001$ (Highly Significant); All parameters show highly significant temporal variation across the 6-month period; General Trend: March < April < May ≤ June = July < August (indicating increasing contamination over time)

Lead rose from 0.090 ± 0.030 to 0.140 ± 0.030 mg/kg (55.6%; $r^2 = 0.967$; $p < 0.001$). At this rate, linear extrapolation would reach the FAO/WHO maximum (0.30 mg/kg) in ~16 months, making the trend relevant to food-safety management despite current values being below the limit (Landrigan et al., 2020).

Arsenic increased by 83.3%, from 0.060 ± 0.030 to 0.110 ± 0.030 mg/kg (r^2 = 0.952; p < 0.001). Copper rose from 1.700 to 2.000 mg/kg (17.6%; r^2 = 0.974), zinc from 44.0 to 49.0 mg/kg (11.4%; r^2 = 0.958), both well within reference values, and iron from 340.0 to 390.0 mg/kg (14.7%; r^2 = 0.958).

The consistent increase across all contaminants, with no reversal or plateau over six months, indicates uptake exceeded depuration during this period; whether this continues requires continued monitoring.

3.7 Physicochemical characteristics of interstitial water

Turbidity differed significantly among stations (Table 7; p < 0.001), declining from 25.38 ± 0.83 FNU at Station 1 to 13.18 ± 0.87 FNU at Station 2 and 10.38 ± 0.87 FNU at Station 3. All exceeded the WHO/DPR guideline (5 NTU), Station 1 by >5-fold. High turbidity increases surface area for contaminant sorption and may reduce photosynthesis in submerged vegetation (ELTurk et al., 2019).

TDS and conductivity did not differ among stations (p > 0.05; TDS 11.06–11.51 mg/L; conductivity 20.11–21.01 µS/cm), but were far lower than expected for brackish water at the reported salinities (8.2–9.0), which would normally correspond to ~10,000–15,000 µS/cm and TDS of several thousand mg/L. Salinity differed significantly (p < 0.05), highest at Station 3 (8.99 ± 0.02), then Station 1 (8.52 ± 0.02) and Station 2 (8.21 ± 0.01); these small differences may affect competitive desorption of metal cations.

Total alkalinity increased downstream (27.83 ± 2.14 to 32.83 ± 2.14 and 35.83 ± 2.14 mg/L; p < 0.01), reflecting bicarbonate accumulation from microbial organic-matter decomposition (Berner, 1980) and more intense downstream diagenesis, consistent with dissolved Fe and Cr patterns.

DO did not differ among stations (5.84 ± 0.16, 6.07 ± 0.18 and 6.08 ± 0.36 mg/L; p > 0.05) and exceeded the DPR minimum (5.0 mg/L), but surface measurements do not capture deeper anoxic layers. BOD_5 increased from 2.82 ± 0.17 to 3.33 ± 0.15 mg/L (p < 0.05), within the DPR limit (10 mg/L), while COD rose from 51.20 ± 1.64 to 56.40 ± 1.34 mg/L (p < 0.01), exceeding the DPR limit (40 mg/L) by 28–41% at all stations. The high COD: BOD_5 ratio indicates recalcitrant organics, probably petroleum-derived aromatics (Samanta et al., 2022).

pH did not differ among stations (7.40 ± 0.01, 7.49 ± 0.00 and 7.50 ± 0.01; p > 0.05) and was within the WHO/DPR range (6.5–8.5). Although near-neutral pH normally limits dissolved metals via hydroxide/carbonate precipitation, persistent Cd and Ni exceedances indicate metal loading exceeded natural attenuation capacity.

Table 7: Mean ± SD interstitial water physicochemical parameters by station.

PARAMETERS	Station 1 (Mean ± SD)	Station 2 (Mean ± SD)	Station 3 (Mean ± SD)	Significance
Turbidity (FNU)	25.38 ± 0.83	13.18 ± 0.87	10.38 ± 0.87	***
TDS (mg/L)	11.51 ± 0.01	11.06 ± 0.01	11.41 ± 0.01	NS
Conductivity (µs/cm)	21.01 ± 0.01	20.11 ± 0.01	20.31 ± 0.01	NS
Salinity (mg/L)	8.52 ± 0.02	8.21 ± 0.01	8.99 ± 0.02	*
Total Alkalinity (mg/L)	27.83 ± 2.14	32.83 ± 2.14	35.83 ± 2.14	**
DO (mg/L)	5.84 ± 0.16	6.07 ± 0.18	6.08 ± 0.36	NS
BOD (mg/L)	2.82 ± 0.17	3.03 ± 0.15	3.33 ± 0.15	*
COD (mg/L)	51.20 ± 1.64	53.40 ± 1.34	56.40 ± 1.34	**
pH	7.40 ± 0.01	7.49 ± 0.003	7.50 ± 0.01	NS

3.8 Temporal variation in interstitial water physiochemistry

Turbidity declined sharply from 25.10 ± 0.22 FNU in March to 12.30 ± 1.92 FNU in April (51%), then recovered gradually to 15.30 ± 3.96 FNU in August (p < 0.001; Table 8), exceeding the 5 NTU guideline in every month. Resuspension during recovery may re-expose the water column and benthic boundary layer to particle-bound contaminants.

TDS and conductivity varied significantly but only slightly (TDS 11.41–11.53 mg/L; p < 0.05), while salinity did not vary (8.39–8.59; p > 0.05), so salinity-driven desorption cannot explain dissolved-metal patterns. Persistent Cd and Ni exceedances therefore reflect sustained release from contaminated sediment under reducing conditions.

Total alkalinity varied significantly ($p < 0.01$), rising from 29.67 mg/L in March to 33.67 mg/L in June, dropping to 26.33 mg/L in July, and recovering to 34.33 mg/L in August. The July depression coincides with peak dry-season tidal energy, which may resuspend and flush diagenetic bicarbonate (Nwankwoala, 2021), while the overall upward trend indicates intensifying anaerobic diagenesis, consistent with increasing tissue metal burdens.

DO also varied ($p < 0.01$), dipping in July (5.77 ± 0.19 mg/L) against increasing values from 5.87 mg/L in March to 6.30 mg/L in August. This July minimum, coinciding with the alkalinity minimum and turbidity recovery, suggests resuspension of oxygen-demanding organic sediment (ELTurk et al., 2019). All values remained above 5.0 mg/L, but with a narrow margin.

BOD_5 and COD did not vary significantly ($p > 0.05$), although COD exceeded the DPR limit of 40 mg/L in every month (52.00–55.00 mg/L). Neither was measured in July, the month most likely to show peak oxygen demand, a gap for future work. pH varied significantly ($p < 0.001$) within a narrow range (7.40–7.51); lower values in March and June may reflect episodic acidic decomposition products, buffered by bicarbonate alkalinity (Berner, 1980).

Table 8: Monthly interstitial water physicochemical parameters (mean ± SD)

PARAMETERS	March	April	May	June	July	August	Significance
Turbidity (FNU)	25.100 ± 0.223	12.300 ± 1.924	12.767 ± 2.031	13.633 ± 2.431	14.433 ± 3.183	15.300 ± 3.963	***
TDS (mg/L)	11.490 ± 0.189	11.407 ± 0.189	11.453 ± 0.189	11.510 ± 0.189	11.520 ± 0.189	11.530 ± 0.189	*
Conductivity (µs/cm)	20.477 ± 0.189	20.390 ± 0.189	20.433 ± 0.189	20.510 ± 0.189	20.520 ± 0.189	20.530 ± 0.189	*
Salinity (mg/L)	8.520 ± 0.365	8.390 ± 0.365	8.520 ± 0.365	8.590 ± 0.365	8.405 ± 0.365	8.540 ± 0.365	NS
Total Alkalinity (mg/L)	29.667 ± 3.055	30.667 ± 2.887	32.667 ± 2.887	33.667 ± 2.887	26.333 ± 3.055	34.333 ± 2.887	**
DO (mg/L)	5.867 ± 0.200	5.967 ± 0.189	6.100 ± 0.189	6.200 ± 0.189	5.767 ± 0.189	6.300 ± 0.189	**
BOD (mg/L)	2.933 ± 0.321	2.933 ± 0.245	3.100 ± 0.245	3.200 ± 0.245	ND	3.000 ± 0.245	NS
COD (mg/L)	52.333 ± 3.055	52.000 ± 2.887	54.000 ± 2.887	55.000 ± 2.887	ND	54.000 ± 2.887	NS
pH	7.41 ± 0.01	7.45 ± 0.003	7.51 ± 0.01	7.40 ± 0.01	7.49 ± 0.003	7.50 ± 0.01	***

Legend: Values represent Mean ± Standard Deviation across samples per month; One-way ANOVA test statistic comparing the six months; ND = No Data / Parameter not measured in that month; Key Findings: TPH, Turbidity, and Cadmium show highly significant temporal variations while DO, show significant changes across months Zinc, and Nickel remain relatively stable throughout the period.

4 DISCUSSION

This study provides a paired record of sediment, porewater and tissue contamination in a petroleum-impacted Niger Delta creek across a dry-to-wet transition. Three findings are central. First, contamination is spatially structured around the most petroleum-affected reach, as shown by TPH, ΣPAH_{16}, Cd and the tissue gradients. Second, hydrocarbon and tissue burdens rose or persisted above reference values across the six months, whereas bulk metals in sediment were temporally stable. Third, dissolved metals and hydrocarbons in porewater exceeded reference values at all stations, a finding that bulk sediment analysis alone would not reveal.

4.1 Spatial structure and source attribution

The peak sediment TPH and ΣPAH_{16} at Station 2, with downstream attenuation, are consistent with a point-source geometry adjacent to petroleum infrastructure (Neff et al., 2011). The co-occurrence of TPH, PAH and Cd peaks at Station 2 is consistent with a common petroleum-related source. Zinc and iron, by contrast, show a broader and less distinctive pattern, which may reflect diffuse inputs and natural geology. Nickel and chromium showed reverse gradients, with higher values upstream. This pattern is more consistent with geogenic background and organic-carbon-controlled retention than with point discharge (Ovutor & Brisibe, 2020).

The contamination found at Station 1, which was selected as an upstream reference, indicates that the reference station is not free of anthropogenic influence. Cadmium and TPH at Station 1 exceeded regional and global background values. The study therefore lacks a truly uncontaminated reference, and comparisons should be interpreted as relative rather than absolute. Future work should sample an upstream location beyond the influence of the Bille infrastructure.

The design does not support causal attribution to any individual operator. The stations are co-located with several facilities, and the study did not apportion sources using isotopic, biomarker or congener-ratio methods. Source apportionment would require such analyses, together with operator discharge records.

4.2 Temporal dynamics and the March pulse

The March interstitial-water TPH pulse (14.36 mg/L) and the March sediment PAH maximum are the most distinctive features of the record. Both are consistent with the reported gas incident immediately before sampling Obi (2021). Acute spills typically produce short-lived peaks in soluble hydrocarbons, followed by partial recovery through microbial degradation and tidal flushing (Turner et al., 2019). The April–August data show that the system did not return to pre-incident levels in some respects, particularly in porewater TPH, which remained about 180 times the reference value used. Continued elevation of tissue cadmium, lead and arsenic after the pulse suggests that exposure through contaminated sediment persisted.

These patterns should be interpreted with the limits of a six-month dataset in mind. Without pre-incident baselines, the study cannot separate the incident's contribution from chronic background loading. Pre-incident data, if available, would substantially strengthen the interpretation.

4.3 Bioavailability and the role of porewater

Porewater data were central to this study. Although bulk sediment Ni, Zn and Cr were below ISQG and ERL thresholds, dissolved Ni exceeded WHO and DPR limits at all stations, reflecting that the freely dissolved fraction, rather than total metal, governs biological uptake (Di Toro et al., 1991). Similar porewater exceedances occur in other Niger Delta and estuarine systems (Okonkwo et al., 2021; ELTurk et al., 2019).

Temporal stability of dissolved Zn and Ni is consistent with sulfide buffering, whereby AVS controls dissolved metals while AVS exceeds simultaneously extracted metals (Di Toro et al., 1992).

Cadmium differed: its mean porewater concentration showed no spatial variation, but episodic April and August pulses reached 33–53 times the WHO guideline. Under the AVS model, Cd would be buffered until AVS exhaustion, after which pulses could occur (Di Toro et al., 1992). Such pulses may arise from organic-rich, sulfide-limited microzones or episodic oxidation, while iron-oxide reduction is an alternative, non-exclusive explanation.

PAHs were undetected in porewater but measurable in sediment and tissue, indicating sediment ingestion, not porewater uptake, was the dominant exposure route in *T. fuscatus*. Porewater-based equilibrium-partitioning models would therefore underestimate exposure in this species (Di Toro et al., 1991).

4.4 Accumulation in *Tympanotonus fuscatus*

Tissue contaminants consistently increased from Station 1 to Station 3, following the sediment gradient, although Station 3 sediment lacked the highest TPH or PAH concentrations. Other factors therefore contributed to exposure at Station 3, including its higher TOC (8.95%), greater fine-sediment deposition, and more intensely reducing conditions favouring metal dissolution (ELTurk et al., 2019). However, sediment grain size and organic content were not measured, limiting this interpretation.

These tissue burdens are directly relevant to human health. Increasing Cd and Pb over six months, with no depuration, is consistent with continuous dietary uptake. Cadmium is nephrotoxic and carcinogenic and is retained in molluscan tissue by metallothioneins (Afiukwa et al., 2020); lead is neurotoxic at low levels, particularly in children (Landrigan et al., 2020). Arsenic speciation is needed to determine carcinogenic risk.

Although current concentrations are below FAO/WHO maxima for molluscs, these limits were designed for seafood in international trade, so their application to subsistence harvesting in a degraded creek requires caution. A formal dietary exposure assessment using local consumption rates and body-weight-normalised intake is therefore needed before health-based conclusions are drawn (Jaja-Chimedza et al., 2022).

4.5 Physicochemical controls

The physicochemical data support the geochemical interpretation. Downstream increases in alkalinity, BOD_5, COD and dissolved iron, together with the decline in turbidity, suggest progressive organic enrichment and intensifying reducing conditions. These conditions favour reductive dissolution of iron oxyhydroxides and release of co-sorbed metals (Chris et al., 2024). The near-neutral pH and stable salinity mean that pH and salinity cannot explain the spatial or temporal patterns in dissolved metals.

Turbidity exceeded the 5 NTU guideline at every station and in every month. This matters both as an aesthetic concern and because particle-bound contaminants can be transported and resuspended. COD exceeded the DPR limit throughout the study, indicating a persistent load of recalcitrant organic material.

The TDS and conductivity values must be treated with caution. They are inconsistent with the salinities reported and cannot be used to draw ionic-strength inferences until verified (Section 3.7).

4.6 Implications for management

The results support immediate, practical actions. Harvest advisories for *T. fuscatus* from the most contaminated reach (Station 3 and the downstream tidal flats) should be considered while a formal dietary exposure assessment is completed. Source control and regulatory enforcement under the Department of Petroleum Resources and the National Environmental Standards and Regulations Enforcement Agency (NESREA, 2011) are needed to address the TPH and PAH burdens in sediment and porewater. Routine monitoring of porewater, not only bulk sediment, should be adopted for regulatory purposes, together with tissue monitoring for Cd, Pb and As. Sediment remediation should target the Station 2 hotspot. The monitoring programme should be extended over multiple seasons, with July porewater data, AVS and grain size included.

5 CONCLUSIONS

Bille Creek sediments, porewater and *T. fuscatus* soft tissue were contaminated with petroleum hydrocarbons and several heavy metals over a six-month period in 2026. Sediment TPH and ΣPAH_{16} peaked at the station closest to petroleum infrastructure, and cadmium exceeded sediment quality guidelines at two stations. Porewater TPH spiked in March, then stabilised above reference values, and dissolved nickel and iron exceeded WHO guideline values at all stations. In *T. fuscatus*, cadmium, lead, arsenic, TPH and ΣPAH increased from the upstream to the downstream station and over time. These results indicate that contamination is spatially structured and temporally persistent, and that the biota harvested for food carry increasing contaminant burdens. Harvest advisories, source control and continued multi-matrix monitoring are warranted. Future work should include source apportionment, chromium and arsenic speciation, AVS measurement, grain-size analysis, a pre-incident baseline and a dietary exposure assessment.

STATEMENTS ON COMPLIANCE WITH ETHICAL STANDARDS

Acknowledgments

The authors thank the fishing communities of Bille Creek for access to sampling sites and the technical staff of the Department of Fisheries, University of Port Harcourt, for laboratory support.

Funding Source

The authors gratefully acknowledge the support received from the TETFund Institutional-Based Research Grant (Grant No. TETF/ES/DR&D/UNIPORT-H/IBR/2025VOL.1:002).

Disclosure of conflict of interest

The authors declare that there is no conflict of interest to be disclosed.

REFERENCES

[1] Abdel-Shafy, H. I., & Mansour, M. S. M. (2016). A review on polycyclic aromatic hydrocarbons: Source, environmental impact, effect on human health and remediation. Egyptian Journal of Petroleum, 25(1), 107–123. https://doi.org/10.1016/j.ejpe.2015.03.011

[2] Afiukwa, C. A., Ogbu, I. S., Nwankwo, N. I., Afiukwa, F. N., Ude, C. M., & Chukwu, C. I. (2020). Bioaccumulation of heavy metals in *Tympanotonus fuscatus* in Cross River Estuary, Nigeria. Journal of Toxicology and Environmental Health Sciences, 12(1), 1–9. https://doi.org/10.5897/JTEHS2019.0404

[3] Ali, H., Khan, E., & Ilahi, I. (2019). Environmental chemistry and ecotoxicology of hazardous heavy metals: Environmental persistence, toxicity, and bioaccumulation. Journal of Chemistry, 2019, Article 6730305. https://doi.org/10.1155/2019/6730305

[4] American Public Health Association (APHA). (2017). Standard methods for the examination of water and wastewater (23rd ed.). APHA.

[5] Barimalaa, I. S., Akonkwa, B. M., & Ndimele, P. E. (2020). Bioaccumulation of heavy metals and polycyclic aromatic hydrocarbons in sediment and *Tympanotonus fuscatus* from an oil-impacted estuary in the Niger Delta, Nigeria. Environmental Science and Pollution Research, 27(18), 22145–22160. https://doi.org/10.1007/s11356-020-08419-7

[6] Berner, R. A. (1980). Early diagenesis: A theoretical approach. Princeton University Press.

[7] Canadian Council of Ministers of the Environment (CCME). (1999). Canadian sediment quality guidelines for the protection of aquatic life: Summary tables. CCME.

[8] Chris, D. I., Wokeh, O. K., Adib, M. N. A. M., Lananan, F., Kassim, M. N. I., & Wei, l. S. (2024). Distribution Of Hadrochemical Parameters, Toxicology and Hazardous Elements Bioaccumulation in Periwinkle (*Tympanotonus fuscatus*) From the Niger Delta Coast, Nigeria. Planetary Sustainability, 2(2), 1-16. https://doi.org/10.46754/ps.2024.07.001%20

[9] Department of Petroleum Resources (DPR). (2002). Environmental guidelines and standards for the petroleum industry in Nigeria (EGASPIN). DPR.

[10] Di Toro, D. M., Mahony, J. D., Hansen, D. J., Scott, K. J., Carlson, A. R., & Ankley, G. T. (1992). Acid volatile sulfide predicts the acute toxicity of cadmium and nickel in sediments. Environmental Science & Technology, 26(1), 96–101. https://doi.org/10.1021/es00025a009

[11] Di Toro, D. M., Zarba, C. S., Hansen, D. J., Berry, W. J., Swartz, R. C., Cowan, C. E., Pavlou, S. P., Allen, H. E., Thomas, N. A., & Paquin, P. R. (1991). Technical basis for establishing sediment quality criteria for nonionic organic chemicals using equilibrium partitioning. Environmental Toxicology and Chemistry, 10(12), 1541–1583. https://doi.org/10.1002/etc.5620101203

[12] Ezemonye, L. I. N., Tongo, I., Enuneku, A. A., Ogbomida, E., & Ogbeide, O. (2021). Risk implications of heavy metal and polycyclic aromatic hydrocarbon contamination of surface sediments in petroleum-impacted estuaries of Edo State, Nigeria. Environmental Geochemistry and Health, 43(2), 761–781. https://doi.org/10.1007/s10653-020-00564-6

[13] FAO/WHO. (2011). Codex general standard for contaminants and toxins in food and feed (CXS 193-1995). Codex Alimentarius Commission.

[14] Förstner, U., & Wittmann, G. T. W. (2012). Metal pollution in the aquatic environment (2nd ed.). Springer. https://doi.org/10.1007/978-3-642-69385-4

[15] Obi, N. (2021). Study of the Impact of gas flaring on the health of communities in Delta region of Nigeria (Doctoral dissertation, Ph. D. dissertation, School of Dentistry & Medical Sciences, Faculty of Science, Charles Sturt University, Sydney, Australia).

[16] Häder, D.-P., Banaszak, A. T., Villafañe, V. E., Narvarte, M. A., González, R. A., & Helbling, E. W. (2020). Anthropogenic pollution of aquatic ecosystems: Emerging problems with global implications. Science of the Total Environment, 713, Article 136586. https://doi.org/10.1016/j.scitotenv.2020.136586

[17] Jaja-Chimedza, A., Graf, B. L., Jingjing, L., Kuhn, P., Raskin, I., & Waterman, I. J. (2022). Dietary exposure and human health risk assessment of polycyclic aromatic hydrocarbons via consumption of shellfish from tropical coastal environments. Food and Chemical Toxicology, 162, Article 112874. https://doi.org/10.1016/j.fct.2022.112874

[18] Landrigan, P. J., Stegeman, J. J., Fleming, L. E., Allemand, D., Anderson, D. M., Backer, L. C., et al. (2020). Human health and ocean pollution. Annals of Global Health, 86(1), Article 151. https://doi.org/10.5334/aogh.2831

[19] Lawson, E. O. (2021). Proximate composition and heavy metal concentrations in the periwinkle *Tympanotonus fuscatus* from Ondo State coastal waters, Nigeria. Journal of Aquatic Food Product Technology, 30(5), 545–556. https://doi.org/10.1080/10498850.2021.1885736

[20] Long, E. R., MacDonald, D. D., Smith, S. L., & Calder, F. D. (1995). Incidence of adverse biological effects within ranges of chemical concentrations in marine and estuarine sediments. Environmental Management, 19(1), 81–97. https://doi.org/10.1007/BF02472006

[21] MacDonald, D. D., Ingersoll, C. G., & Berger, T. A. (2000). Development and evaluation of consensus-based sediment quality guidelines for freshwater ecosystems. Archives of Environmental Contamination and Toxicology, 39(1), 20–31. https://doi.org/10.1007/s002440010075

[22] Masindi, V., & Muedi, K. L. (2018). Environmental contamination by heavy metals. In H. E. M. Saleh & R. F. Aglan (Eds.), Heavy metals (pp. 115–133). IntechOpen. https://doi.org/10.5772/intechopen.76082

[23] Ndome, C. B., Ekwu, A. O., & Atata, R. F. (2012). Heavy metal content of some commercially important fishes of the Cross River Estuary and the potential health risks to human consumers. American Journal of Food and Nutrition, 2(1), 18–25. https://doi.org/10.5251/ajfn.2012.2.1.18.25

[24] Neff, J. M., Lee, K., & DeBlois, E. M. (2011). Produced water: Overview of composition, fates, and effects. In K. Lee & J. Neff (Eds.), Produced water: Environmental risks and advances in mitigation technologies (pp. 3–54). Springer. https://doi.org/10.1007/978-1-4614-0046-2_1

[25] National Environmental Standards and Regulations Enforcement Agency (NESREA). (2011). National environmental (surface and groundwater quality) regulations. Federal Government of Nigeria.

[26] Nriagu, J., Udofia, E. A., Ekong, I., & Ebuk, G. (2016). Health risks associated with oil pollution in the Niger Delta, Nigeria. International Journal of Environmental Research and Public Health, 13(3), Article 346. https://doi.org/10.3390/ijerph13030346

[27] Nwankwoala, H. O. (2021). Hydrogeology and groundwater resources in the Niger Delta: An assessment of environmental challenges and management strategies. Journal of Water Resource and Protection, 13(4), 292–316. https://doi.org/10.4236/jwarp.2021.134017

[28] Nwipie, G. N., Wegwu, M. O., & Ogbonnia, E. N. (2019). Bioaccumulation and public health implications of heavy metals in *Tympanotonus fuscatus* from Okirika, Rivers State, Nigeria. International Research Journal of Public and Environmental Health, 6(4), 70–77. https://doi.org/10.5897/IRJPEH2018.0367

[29] Obeka, A. C., & Numbere, A. O. (2020). The impact of oil exploration on aquatic biodiversity in the Niger Delta. Journal of Applied Sciences and Environmental Management, 24(7), 1265–1272. https://doi.org/10.4314/jasem.v24i7.23

[30] Ovutor, E. J., & Brisibe, E. A. (2020). Environmental impact of gas flaring on vegetation and air quality in oil-producing communities of the Niger Delta. International Journal of Environmental Studies, 77(3), 487–498. https://doi.org/10.1080/00207233.2019.1686558

[31] R Core Team. (2023). R: A language and environment for statistical computing. R Foundation for Statistical Computing, Vienna, Austria. https://www.R-project.org

[32] Readman, J. W., Fillmann, G., Tolosa, I., Bartocci, J., Villeneuve, J. P., Catinni, C., & Mee, L. D. (2002). Petroleum and PAH contamination of the Black Sea. Marine pollution bulletin, 44(1), 48-62. https://doi.org/10.1016/S0025-326X(01)00189-8

[33] Samanta, P., Pal, S., Mukherjee, A. K., & Ghosh, A. R. (2022). Polycyclic aromatic hydrocarbons in the environment: A review of occurrence, distribution, accumulation, fate, and biological effects. Environmental Geochemistry and Health, 44(10), 3561–3588. https://doi.org/10.1007/s10653-021-01133-z

[34] ELTurk, M., Abdullah, R., Zakaria, R. M., & Bakar, N. K. A. (2019). Heavy metal contamination in mangrove sediments in Klang estuary, Malaysia: Implication of risk assessment. Estuarine, Coastal and Shelf Science, 226, 106266. https://doi.org/10.1016/j.ecss.2019.106266

[35] Shapiro, S. S., & Wilk, M. B. (1965). An analysis of variance test for normality (complete samples). Biometrika, 52(3–4), 591–611. https://doi.org/10.1093/biomet/52.3-4.591

[36] Turner, R. E., Overton, E. B., Meyer, B. M., Miles, M. S., McClenachan, G., Hooper-Bùi, L., Engel, A. S., Koch, B. J., Shaw, J. L., Chen, Q., & Milan, C. S. (2019). Distribution and recovery trajectory of Macondo (Mississippi Canyon 252) oil in Louisiana coastal wetlands. Marine Pollution Bulletin, 145, 15–25. https://doi.org/10.1016/j.marpolbul.2019.05.028

[37] Ugochukwu, C. N. C., & Lall, U. (2019). The impact of oil pollution on the sustainable development of the Niger Delta. In Environmental pollution from petroleum products. IntechOpen. https://doi.org/10.5772/intechopen.88490

[38] United States Environmental Protection Agency (USEPA). (2007). SW-846 test methods for evaluating solid waste: Physical/chemical methods (3rd ed.). USEPA.

[39] United States Environmental Protection Agency (USEPA). (2014). Priority pollutants list. USEPA.

[40] United States Environmental Protection Agency (USEPA). (2023). Regional screening levels (RSLs) for chemical contaminants at Superfund sites. USEPA. https://www.epa.gov/risk/regional-screening-levels-rsls-generic-tables

[41] Vane, C. H., Kim, A. W., Emmings, J. F., Turner, G. H., Moss-Hayes, V., & Richardson, N. (2020). Grain size and organic matter controls on polycyclic aromatic hydrocarbon (PAH) and heavy metal contamination of surface sediments in the Mersey Estuary, United Kingdom. Marine Pollution Bulletin, 161(Part B), Article 111810. https://doi.org/10.1016/j.marpolbul.2020.111810

[42] World Health Organization (WHO). (2022). Guidelines for drinking-water quality (4th ed., incorporating the first and second addenda). WHO.